SLURP-1 Modulates Corneal Homeostasis by Serving as a Soluble Scavenger of Urokinase-Type Plasminogen Activator

Sudha Swamynathan[1] and Shivalingappa K. Swamynathan[1–3]

[1]Department of Ophthalmology, University of Pittsburgh School of Medicine, Pittsburgh, Pennsylvania, United States
[2]McGowan Institute of Regenerative Medicine, University of Pittsburgh, Pittsburgh, Pennsylvania, United States
[3]Department of Cell Biology, University of Pittsburgh School of Medicine, Pittsburgh, Pennsylvania, United States

Correspondence: Shivalingappa K. Swamynathan, University of Pittsburgh School of Medicine, Eye and Ear Institute, 203 Lothrop Street, Room 1025, Pittsburgh, PA 15213,USA; swamynathansk@upmc.edu.

Submitted: June 25, 2014
Accepted: August 15, 2014

Citation: Swamynathan S, Swamynathan SK. SLURP-1 modulates corneal homeostasis by serving as a soluble scavenger of urokinase-type plasminogen activator. *Invest Ophthalmol Vis Sci*. 2014;55:6251–6261. DOI: 10.1167/iovs.14-15107

Purpose. Our previous study revealed the immunomodulatory property of the secreted lymphocyte antigen (Ly6)/urokinase-type plasminogen activator receptor (uPAR)-related protein-1 (SLURP1), abundantly expressed in the cornea and associated with the hyperkeratotic disorder Mal de Meleda. Here, we test the hypothesis that SLURP1 modulates the functions of membrane-tethered uPAR by acting as a soluble scavenger of its ligand urokinase-type plasminogen activator (uPA).

Methods. Human corneal limbal epithelial (HCLE) and mouse corneal stromal fibroblast MK/T-1 cells were employed to examine the effect of SLURP1 on cell proliferation and migration. Human corneal limbal epithelial cell clones stably expressing SLURP1 under the control of cytomegalovirus (CMV) promoter were generated using lentiviral vectors. Recombinant 6× His-mouse Slurp1 and maltose-binding protein (MBP)-mouse uPA were expressed in *Escherichia coli* and partially purified using nickel-ion and amylose columns, respectively. Slurp1 interaction with uPA was detected using ligand blots, ELISA, pull-down assays, and immunofluorescent staining.

Results. Stable expression of SLURP1 in HCLE cells was confirmed by immunoblots and immunofluorescent staining. Human corneal limbal epithelial and MK/T-1 cell proliferation and migration rates were suppressed by exogenous SLURP1. Ligand blots, ELISA, and pull-down assays indicated that Slurp1 efficiently interacts with uPA. Immunofluorescent staining demonstrated that exogenous SLURP1 decreased the amount of cell surface–bound uPA in the leading edges of migrating cells. In gap-filling assays, wild-type HCLE cells responded to uPA by increasing their velocity and closing larger area, while the SLURP1-expressing HCLE cells failed to do so.

Conclusions. SLURP1 modulates corneal homeostasis by serving as a soluble scavenger of uPA and regulating the uPA-dependent functions of uPAR.

Keywords: Slurp1, cornea, urokinase, uPA, uPAR, migration, ocular surface

Transparent cornea is an essential component of the optical axis that allows incident light to reach the retina. Being externally exposed, the cornea is subject to frequent, mild, chemical, biological, and physical insults. Recurrent inflammatory response to such insults is potentially blinding. The cornea, however, is "immune privileged" and employs multiple mechanisms to suppress inflammation upon exposure to mild insults.[1–3] It also retains "immune competence," which allows protective inflammation in response to severe insults.[1–3] The delicate balance between corneal immune privilege and competence is governed by a variety of molecules[1–14] that maintain immune quiescence in normal situations and allow inflammation in response to acute infections and injury. Our previous work demonstrated that the secreted lymphocyte antigen (Ly-6)/urokinase-type plasminogen activator receptor-related protein-1 (SLURP1) is a constitutive component of corneal immune privilege that inhibits leukocytic infiltration into the cornea in response to mild insults and is rapidly downregulated when the cornea becomes infected, permitting protective inflammation to develop.[15]

SLURP1 is a member of the Ly6 superfamily characterized by the three-finger fold structure.[16–18] SLURP1 is expressed in a variety of cells including immune cells,[19] bronchial epithelial cells,[20] primary sensory neurons,[21] the skin, exocervix, gums, stomach, trachea and esophagus,[22] oral keratinocytes,[23] and the cornea,[24] and secreted into plasma, saliva, sweat, urine, and tears.[25] Mutations or deletions in *SLURP1* are associated with Mal de Meleda, an autosomal recessive inflammatory disorder characterized by palmoplantar keratoderma and transgressive keratosis.[22,25,26,28–33] *Slurp1* is one of the most abundant transcripts in the neonatal and the adult mouse corneas[24] and is sharply downregulated in the *Klf4* conditional null (*Klf4*CN) corneas that display epithelial fragility, loss of epithelial barrier function, and stromal edema.[26–28] *Slurp1* is rapidly downregulated in several proinflammatory conditions including asthmatic lungs,[29] corneal neovascularization,[30] Barrett's esophagus, adenocarcinomas, malignant melanomas, cervical cancer, and

oral squamous cell carcinomas (NCBI GEO Accession Numbers GSE23347, GDS1321, GDS3472, GDS1375, and GDS1584) consistent with its role as an immunomodulatory molecule. Being structurally similar to α-bungarotoxin, SLURP1 serves as a ligand for α7-nicotinic acetylcholine receptor (α7nAchR),[22,31] regulating immune response, cell adhesion, signal transduction, and tobacco nitrosamine-induced malignant transformation of oral cells through cholinergic pathways.[16,19,23,32,33] The mechanisms by which SLURP1 functions as an immunomodulatory molecule in the cornea have not been studied previously.

The urokinase-type plasminogen activator receptor (uPAR, also known as urokinase receptor or CD87) is another important member of the Ly6 family that plays an integral role in cell survival, proliferation, motility, and invasion.[34] Urokinase-type plasminogen activator receptor contains three direct repeats of the Ly6 domain connected by short linkers and is tethered to cell membrane by glycosyl phosphatidylinositol (GPI)-anchor. Expression of uPAR is limited in quiescent conditions and is upregulated in response to stress, injury, and inflammation, which require active extracellular matrix (ECM) remodeling. Many functions of uPAR are dependent on its interaction with a large number of ligands including urokinase-type plasminogen activator (uPA, also known as urokinase), vitronectin, and integrins. Urokinase-type plasminogen activator receptor regulates cell signaling and ECM proteolysis by localizing uPA to cell surface.[34] Considering the structural similarities between uPAR and SLURP1, we hypothesized that SLURP1 modulates the functions of membrane-tethered uPAR by acting as a soluble scavenger of its ligand uPA. Here, we present evidence that SLURP1 interacts efficiently with uPA, resulting in a reduced rate of cell proliferation and migration.

Materials and Methods

Generation of SLURP1-Expressing Adenoviral and Lentiviral Vectors, and Human Corneal Limbal Epithelial (HCLE)-Stable Clones

Adenoviral vectors expressing Slurp1 were generated in HEK293 cells as before,[15] using AdenoX expression system (Serotype-5; Clontech Laboratories, Mountain View, CA, USA). Sequence-verified human *SLURP1* cDNA in expression vector obtained from CCSB-Broad Lentiviral Vector Library was used to generate lentiviral vectors by transfection of four plasmids (expression plasmid pLX304-Blast-V5-SLURP1[35] [Fisher Scientific, Pittsburgh, PA, USA], pMD2.g [VSVG], pRSV-REV, and pMDLg/pRRE) into 293-FT cells using FuGene 6 transfection reagent (Roche Diagnostic Corp., Indianapolis, IN, USA). Culture media from transfected cells was collected 48 hours after transfection and passed through 0.45-μm filters to isolate the viral particles. Human corneal limbal epithelial[36] cells were infected with lentiviral particles carrying *SLURP1* gene under the control of CMV promoter. Two days after infection, cells were plated at low density and subjected to blasticidin selection for 2 weeks. Individual clones that survived blasticidin selection were propagated further and screened by immunoblots for SLURP1 expression.

Immunoblots

Equal amounts of total protein extracted using M-PER reagent and quantified by bicinchoninic acid method (Pierce, Rockford, IL, USA) were electrophoresed in sodium dodecyl sulfate-polyacrylamide gels, transferred to polyvinylidene difluoride (PVDF) membranes and subjected to immunoblot analysis with 1:1000 dilution of goat anti-human SLURP1 primary antibody (Santa Cruz Biotechnology, Santa Cruz, CA, USA), and 1:1000 dilution of horseradish peroxidase (HRP)–coupled donkey anti-goat IgG secondary antibody (Santa Cruz Biotechnology). Immunoreactive bands were detected by chemiluminescence using Super Signal West Pico solutions (Pierce), exposure of the processed blots to x-ray films, and developing in a standard x-ray film developer.

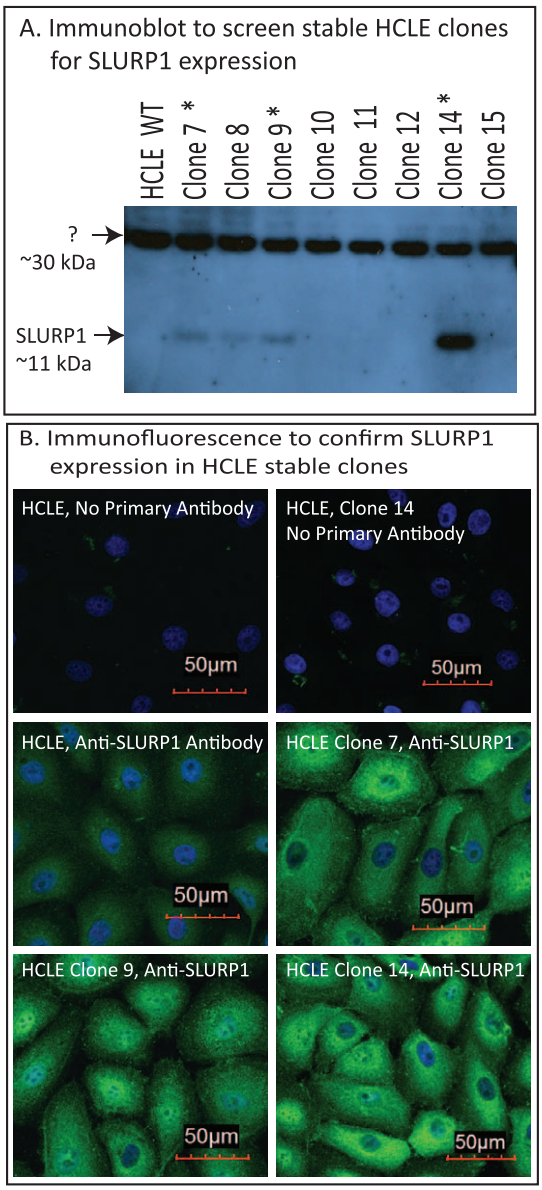

Figure 1. Stable expression of SLURP1 in HCLE cells. HCLE cells stably transduced with lentiviral particles containing *SLURP1* gene under the control of CMV promoter were selected by blasticidin resistance. (**A**) We screened approximately 15 stably transduced single cell–derived clones by immunoblot with anti-SLURP1 antibody. Immunoblot comparison of the expression of SLURP1 in parental HCLE cells with that of eight HCLE-SLURP1 clones identified clones 7, 8, 9, and 14 as expressing SLURP1, with clone 14 being the best. A nonspecific, cross-reacting protein migrating at approximately 30 kDa served as a control for uniformity in protein loading in this gel. (**B**) Immunofluorescent staining of HCLE, HCLE–SLURP1-7, -9, and -14 with anti-SLURP1 antibody confirmed SLURP1 expression in these cells. No primary antibody controls are shown for HCLE and HCLE–SLURP1-14, confirming that the green fluorescence is specific to SLURP1-producing cells.

Investigative Ophthalmology & Visual Science

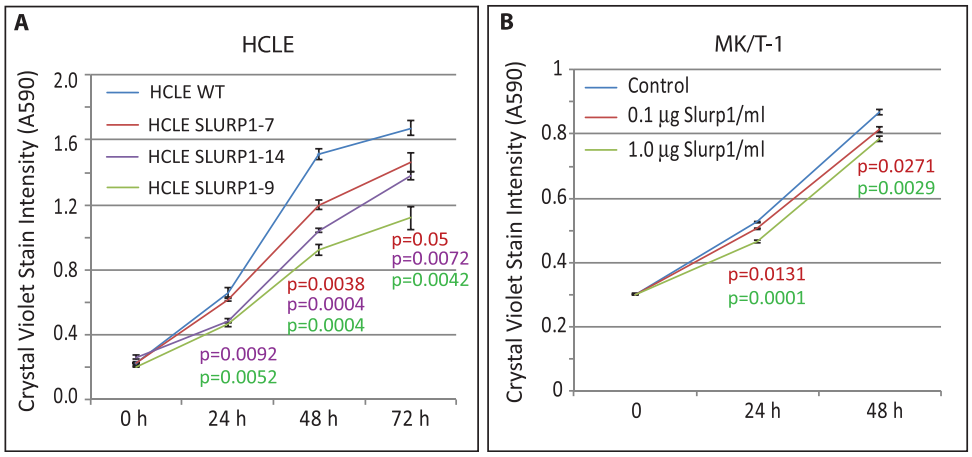

Figure 2. Effect of SLURP1 on cell proliferation. (**A**) SLURP1 inhibits HCLE cell proliferation. Equal numbers of HCLE, or stably transduced HCLE-SLURP1 cells were seeded in 96-well plates, and their densities were monitored at 0, 24, 48, and 72 hours by crystal violet staining and measuring the absorbance at 590 nm. Human corneal limbal epithelial–SLURP1 cells proliferated at a significantly slower pace compared with the parental HCLE cells. (**B**) Slurp1 inhibits MK/T-1 cell proliferation. Equal numbers of MK/T-1 cells were seeded in a tissue culture–treated 96-well plate. One set was removed for staining 4 hours after plating (0 hours). For the rest, Slurp1 was added at 0, 0.1, or 1 µg/mL in 100 µL medium with 5% fetal bovine serum (FBS). Cells were fixed and stained with crystal violet at appropriate times and absorbance measured at 590 nm, as above. Exogenous application of mouse Slurp1 suppressed MK/T-1 cell proliferation in a dose-dependent manner. Statistical significance was determined by Student's *t*-test, and the *P* values for comparison between control and different treatments are provided (*color coordinated with the corresponding trend-lines*) at each time point, when significant.

Cell Proliferation Assays

Mouse corneal stromal fibroblast MK/T-1,[37] HCLE,[36] or HCLE-SLURP1 cells were seeded (10,000 cells per well) in quadruplicate tissue culture–treated 96-well plates. Mouse corneal stromal fibroblast MK/T-1 cells were treated with control maltose-binding protein (MBP), or MBP-Slurp1. Non-adherent cells were removed after 4 hours of plating, which was set as 0 hours. At 0, 24, 48, and 72 hours, the cells were fixed and stained with crystal violet solution (0.2% crystal violet in 10% ethanol) for 15 minutes. Unbound crystal violet was removed by rinsing with distilled water, and cells were subsequently air dried. Crystal violet, which binds DNA, was eluted from cells with 20% acetic acid, and the absorbance measured at 590 nm using Biotek Synergy-II plate reader (Winooski, VT, USA).

Ligand Blots

Ligand blots were performed following the method described by Connolly et al.[38] with minor modifications. We chose mouse kidney, which expresses Slurp1 and many uPAR ligands and offers the advantage of relatively abundant tissue availability, to screen for Slurp1-interacting proteins. Adult mouse kidney lysates were prepared using either homemade lysis buffer (20 mM Tris-HCl, pH 8.0; 150 mM NaCl; 1 mM PMSF; 0.25% Tween-20) or M-PER (Pierce), a nondenaturing commercial detergent formulation that extracts soluble protein. Kidney lysate was separated by nondenaturing PAGE, transferred to nitrocellulose membrane, blocked with 5% milk in phosphate buffered saline (pH 7.4) with 0.1% Tween-20 detergent (PBST), incubated with BSA or partially purified His-Slurp1 (expressed in *E. coli*), and probed with anti-Slurp1 antibody. After the Slurp1-bound proteins were detected, the blot was stripped and reprobed with anti-uPA antibody (Santa Cruz Biotechnology). The blots were then aligned to detect overlapping bands.

ELISAs

High-binding capacity ELISA plates were coated with control MBP, MBP-Slurp1, recombinant human SLURP1, or BSA and blocked with 5% milk. MBP or MBP-uPA fusion protein, mock-cleaved MBP or cleaved MBP-uPA, mouse kidney lysate, or recombinant human uPA was layered on coated surface, washed thoroughly, and the bound uPA was detected using anti-uPA antibody, appropriate HRP-conjugated second antibody, and color-developing reagents.

Pull-Down Assays

Negative control MBP-Slurp1 (expressed in *E. coli* using the vector pMalC2 [New England Biolabs, Ipswich, MA, USA], purified through amylose resin) or His-Slurp1 (expressed in *E. coli* using the vector pTrc His-B [Invitrogen, Carlsbad, CA, USA]) was bound on Ni-ion resin, incubated with adult mouse kidney lysate (as a source of uPA). After thorough washing, His-Slurp1 bound Ni-ion beads were directly placed in Laemmli buffer and heated for sample preparation. The released proteins were then separated by SDS-PAGE and transferred to nitrocellulose membranes. Slurp1-bound uPA was then detected by immunoblot using anti-uPA antibody (Santa Cruz Biotechnology).

Gap-Filling Assays

A scrape wound was introduced in confluent HCLE[36] or HCLE-SLURP1 cells grown on tissue culture–treated plastic wells using a 200-µL pipette tip. Six areas of the gaps were marked underneath the plates and photographed soon after generating the gap (0 hours) and 18 hours later, using a Nikon TS100 inverted microscope (Nikon, Melville, NY, USA) with a 2× objective and a Spot RT camera (Diagnostics Instruments, Sterling Heights, MI, USA). That the same sets of cells were photographed at 0 and 18 hours post gap formation was assured by aligning them with the mark at the bottom of the plates. Initial (0 hours) and unfilled gap areas at 18 hours after wounding were determined using MetaMorph software (Molecular Devices, Sunnyvale, CA, USA). Alternatively, live-cell microscopy was performed using a mechanical stage equipped with a humidified mini-incubator set to 37°C and 5% CO_2. For determining the effect of uPA on gap filling in HCLE and HCLE-SLURP1 cells, recombinant human uPA was added at 50 U/mL

Investigative Ophthalmology & Visual Science

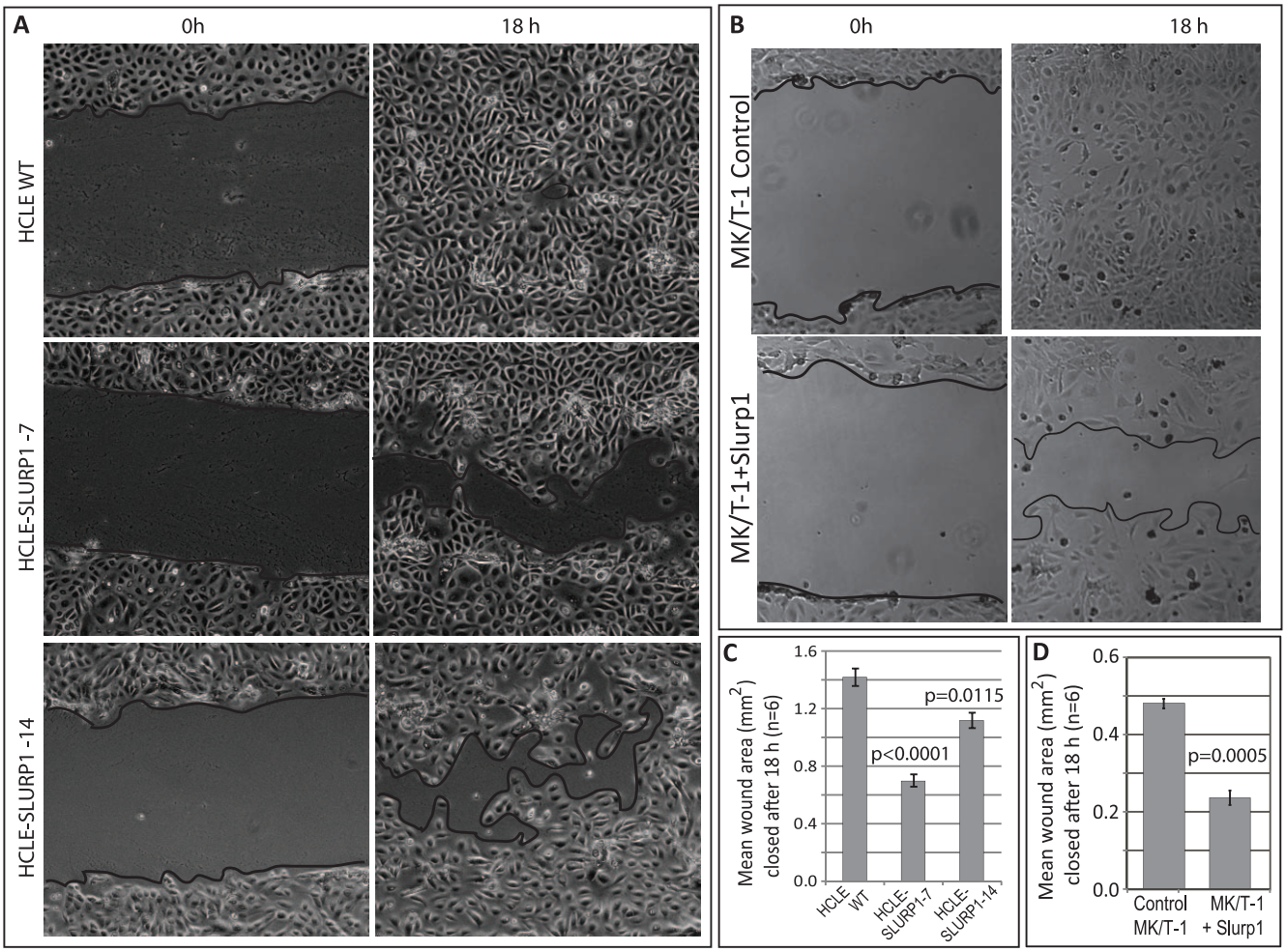

Figure 3. Inhibitory effect of SLURP1 on in vitro gap filling. (**A**) Effect of SLURP1 on HCLE cell migration in gap-filling assays. A gap was introduced in confluent HCLE, HCLE–SLURP1-7 and -14 cells with a 200-μL pipette tip. Gap filling by migration was monitored at 0, and 18 hours post gap generation. Note that a large gap remains open in HCLE–SLURP1-7 and -4 cells, while the gap in control wild-type HCLE cells is completely filled by 18 hours. (**B**) Effect of Slurp1 on MK/T-1 cell migration. Mouse corneal stromal fibroblast MK/T-1 cells were infected with either 2× Tet-Off helper adenovirus (control), or 1× each of Slurp1-expressing adenovirus and Tet-Off helper adenovirus (+Slurp1). One day later, when the cells were confluent, a gap was generated with a 200-μL pipette tip. Gap filling by migration was monitored at 0 and 18 hours post gap generation. Note that by 18 hours, roughly 50% of the gap remained open in cells infected with Slurp1-expressing adenovirus, while the gap in control virus–infected cells is completely filled. (**C**, **D**) Effect of SLURP1 on mean gap area closed after 18 hours, calculated from six different regions in HCLE or MK/T-1 cells. Statistical significance was determined by Student's *t*-test, and the *P* values for comparison between control and different treatments is provided.

culture medium, and the cells were tracked up to 40 hours post gap generation using live-cell microscopy. For studying the effect of Slurp1 on gap filling in MK/T-1 cells, subconfluent MK/T-1 cells were exposed to Slurp1 by infecting with 1× each of Slurp1-expressing adenovirus and Tet-Off helper adenovirus (Slurp1) vectors, or 2× Tet-Off helper adenovirus (control). One day later, when the cells were confluent, a gap was generated with a 200-μL pipette tip. Imaging and analysis of gap filling was performed as above at 0 and 18 hours after generating the gap.

Immunofluorescent Staining of Cell Surface–Bound uPA on HCLE and MK/T-1 Cells

A gap was introduced in confluent HCLE or HCLE-SLURP1 cells grown on vitronectin-coated coverslips, and MK/T-1 cells[37] grown on collagen-coated coverslips. Human corneal limbal epithelial and HCLE-SLURP1 cells were treated with uPA for 4 hours following gap generation and immunofluorescent staining performed with rabbit anti-uPA antibody. In MK/T-1 cells, Slurp1/control protein was added with or without uPA for 4 hours following gap generation, and uPA was detected by immunofluorescent staining with rabbit anti-uPA antibody as above.

Statistical Analyses

All experiments reported here were repeated at least three times, and representative data are presented. In graphs, mean values derived using data from at least three independent repetitions are presented along with standard error bars. Statistical significance was analyzed using Student's *t*-test. Differences between treatments were deemed statistically significant when *P* values were less than 0.05.

Results

Expression of SLURP1 in HCLE Cells

As most cultured cells do not express detectable amounts of SLURP1, we decided to examine the effects of SLURP1

Investigative Ophthalmology & Visual Science

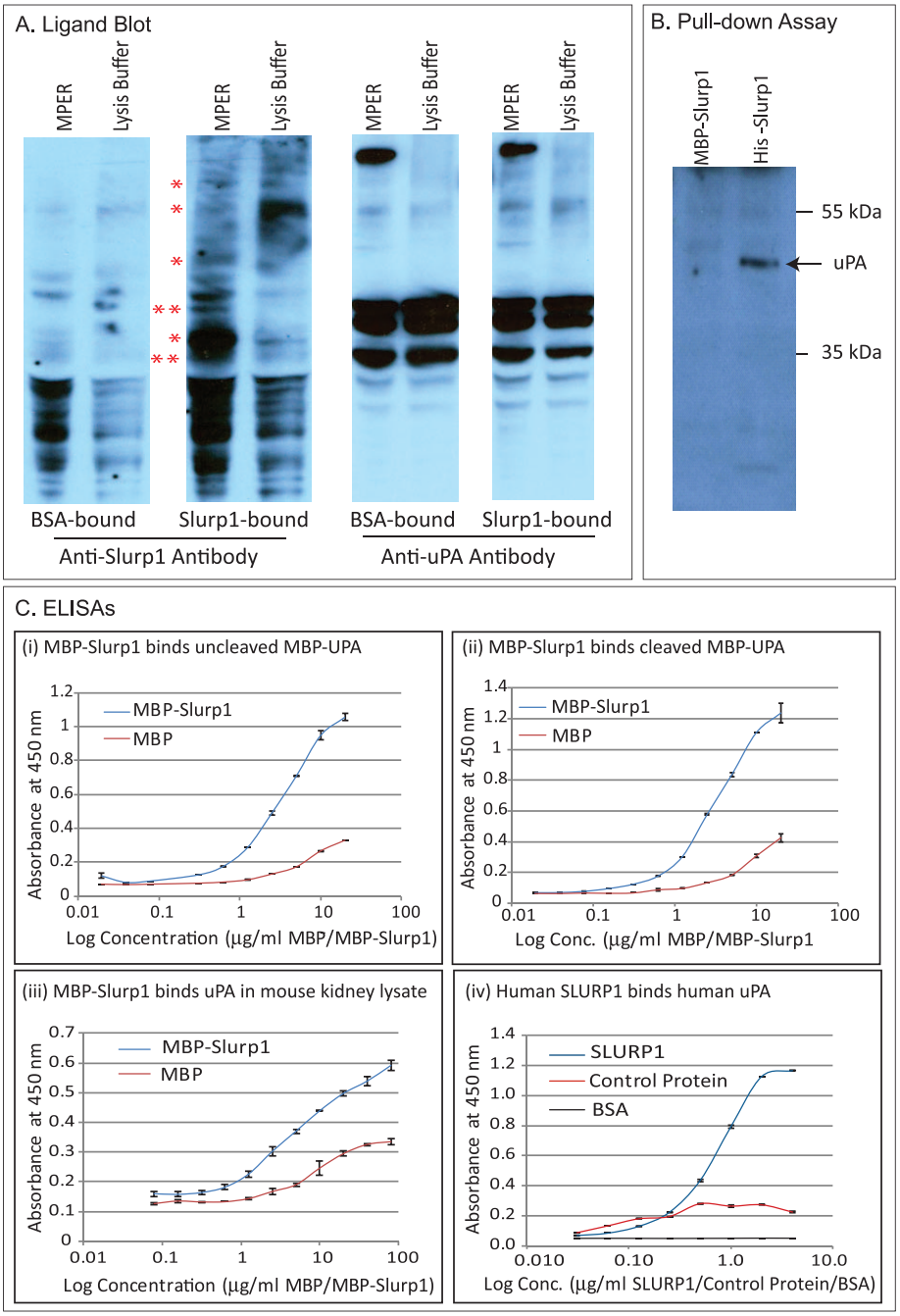

Figure 4. SLURP1 interacts with uPA. (**A**) Ligand-binding assay to identify Slurp1-interacting proteins. Kidney lysates were prepared using either homemade lysis buffer (20 mM Tris-HCl (pH 8.0), 150 mM NaCl, 1 mM PMSF, 0.25% Tween-20), or M-PER (a nondenaturing commercial detergent formulation that extracts soluble protein). Kidney lysates were separated by nondenaturing PAGE, transferred to nitrocellulose membrane, blocked with 5% milk in PBST, incubated with BSA or partially purified His-Slurp1 (expressed in *E. coli*), and probed with anti-Slurp1 antibody. Protein bands that interacted with Slurp1 are indicated by *. These blots were then stripped of the antibody, reprobed with anti-uPA antibody, and aligned with each other to detect overlapping bands (indicated by **). (**B**) Pull-down assay. (1) Negative control MBP-Slurp1 (expressed in *E. coli*, purified through amylose resin) or (2) His-Slurp1 (expressed in *E. coli*) was bound on Ni-ion resin, incubated with kidney lysate (as a source of uPA), washed thoroughly; then bound proteins were separated by SDS-PAGE and Slurp1-bound uPA detected by anti-uPA antibody. (**C**) ELISAs. ELISA plates were coated with MBP or MBP-Slurp1 (i–iii) or recombinant human SLURP1, control protein or BSA (iv), and blocked with 5% milk. Maltose-binding protein (MBP) or MBP-uPA fusion protein (i), mock-cleaved MBP or cleaved MBP-uPA (ii), mouse kidney lysate, or (iii) recombinant human uPA (iv) was layered on coated surface, washed thoroughly, and the bound uPA detected using anti-uPA antibody. Mean values from three repetitions are plotted. *Error bars* represent SEM. Note that in each case, increasing amounts of uPA were detected on SLURP1-coated surface compared with the corresponding controls.

Investigative Ophthalmology & Visual Science

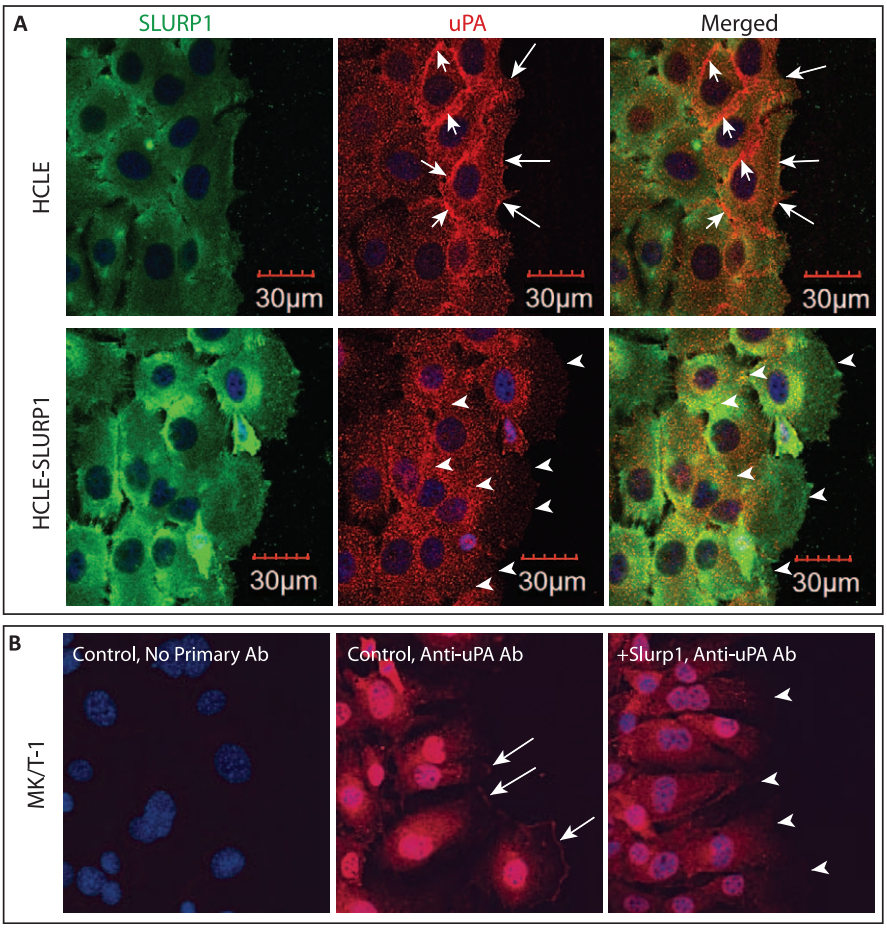

Figure 5. Slurp1 decreases the amount of cell surface–bound uPA at the leading edge. (**A**) Immunofluorescent staining with anti-SLURP1 or anti-uPA antibody was performed after 4 hours of gap formation in confluent HCLE or HCLE-SLURP1 cells grown on vitronectin-coated coverslips and treated with 50 U/mL recombinant human uPA. Note that relatively more uPA is detected in HCLE cells in the intercellular margins (*short arrows*) and the migrating edge (*long arrows*) compared with the HCLE-SLURP1 cells (*arrowheads*). (**B**) Immunofluorescent staining with anti-uPA antibody in MK/T-1 cells plated on collagen-coated coverslip. For detecting uPA in migrating cells, gaps were generated in confluent MK/T-1 cells, which were then treated with uPA and either control protein or partially purified Slurp1 for 4 hours. Cell surface–bound uPA was then detected by immunofluorescent staining with rabbit anti-uPA antibody. Note that relatively more uPA is detected at the moving edge in control protein–treated cells (*long arrows*) compared with those treated with Slurp1 (*arrowheads*).

overexpression in HCLE cells for studying its cellular functions. Following transduction with a SLURP1-expressing lentiviral vector, we screened several blasticidin-resistant single cell–derived clones for SLURP1 expression and identified clones HCLE–SLURP1-7, -9, and -14 for further analyses (Fig. 1A). Efficient overexpression of SLURP1 in these cells was confirmed by immunostaining, which also revealed that SLURP1 is mostly localized in the cytoplasm, and that SLURP1 expression is highest in HCLE–SLURP1-14 cells, consistent with the immunoblots (Fig. 1B).

SLURP1 Suppresses Cell Proliferation

In order to study the effect of SLURP1 on proliferation, equal numbers of wild-type HCLE, HCLE–SLURP1-7, -9, or -14 cells were seeded in 96-well plates, and their densities were monitored at 0, 24, 48, and 72 hours by crystal violet staining. All three HCLE-SLURP1 clones proliferated at a significantly slower pace compared with the parental HCLE cells (Fig. 2A). Though HCLE–SLURP1-7, -9, and -14 produce vastly different amounts of SLURP1 (Fig. 1), a corresponding difference in their suppressive effect on HCLE cell proliferation was lacking, suggesting that a slight increase in SLURP1 expression is enough to cause a large effect on HCLE cell proliferation, and that higher amounts of SLURP1 do not have linear, dose-dependent effects. It is possible that other cofactors (not being overexpressed) are necessary for maximal and/or linear effects of SLURP1. Consistent with these results, mouse corneal stromal fibroblast MK/T-1 cells treated with MBP-Slurp1 proliferated at a significantly slower pace compared with those treated with MBP alone (Fig. 2B). Together, these results suggest that SLURP1 has a suppressive effect on cell proliferation.

Effect of SLURP1 on Cell Migration

We tested the effect of SLURP1 on HCLE cell migration by in vitro gap-filling assays. A gap was introduced in confluent HCLE, HCLE–SLURP1-7 and -14 cells using a 200-μL pipette tip. Gap filling by migration of neighboring cells was monitored at 0 and 18 hours post gap generation. While the gap in control wild-type HCLE cells was completely filled by 18 hours, a large gap remained open in HCLE–SLURP1-7 and -14 cells (Fig. 3A). A similar inhibitory effect of Slurp1 was observed in MK/T-1 cells infected with Slurp1-expressing adenovirus compared with those infected with Tet-Off helper adenovirus alone (Fig. 3B). Measurement of the mean gap area from six different regions in each cell type at 0 and 18

Investigative Ophthalmology & Visual Science

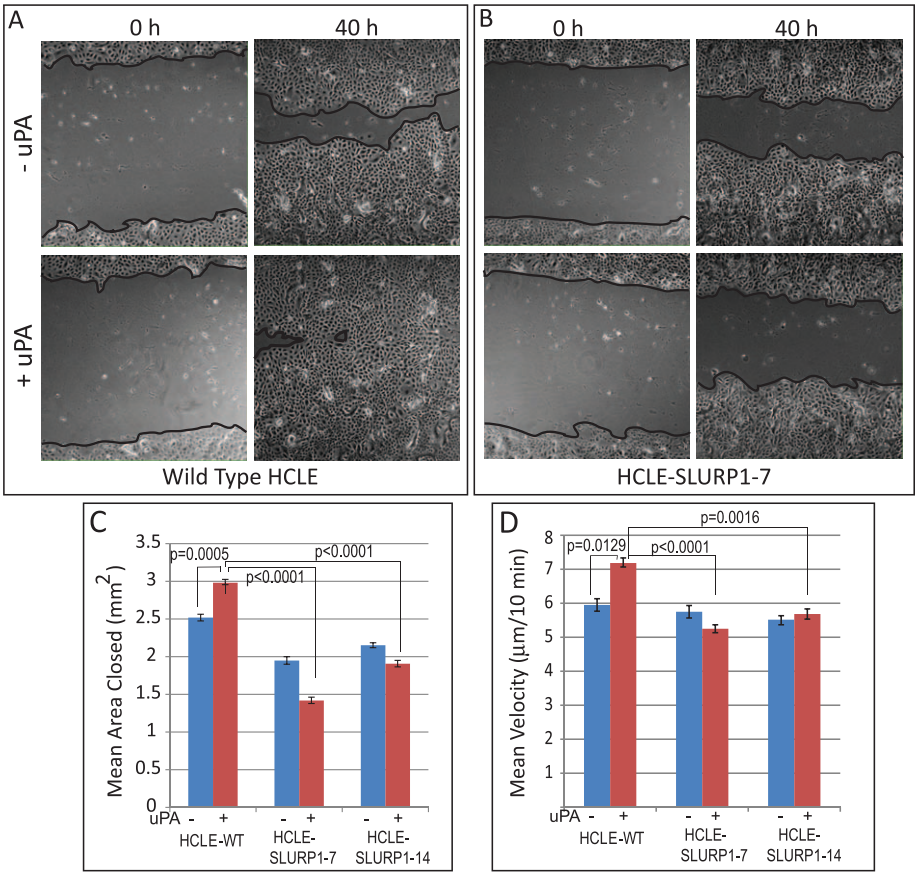

Figure 6. SLURP1 blocks the stimulatory effect of uPA on HCLE cell migration. (**A** and **B**) Gap-filling assay was performed with wild-type HCLE, HCLE–SLURP1-7, and HCLE–SLURP1-14 cells in the presence or absence of recombinant human uPA (50 U/mL). Representative images from wild-type HCLE (**A**) and HCLE–SLURP1-7 (**B**) are shown at 0 and 40 hours after gap formation. Live cell microscopy was used to track the migrating cells in six different regions for 40 hours after gap formation (data presented in Supplemental Video 1). MetaMorph software was used to calculate the mean area closed after 40 hours of gap formation ([**C**]; $n = 6$) and the mean velocity of their migration based on 10 randomly selected cells in each cell type ([**D**]; $n = 10$). While HCLE cells responded to uPA by increasing their mean velocity of migration, HCLE–SLURP1-7 and HCLE–SLURP1-14 cells did not, suggesting that SLURP1 blocks the stimulatory effect of uPA on HCLE cell migration. *Error bars* represent SEM. After cross-comparison, *P* values are only shown where significant.

hours indicated that HCLE–SLURP1-7 and -14 were roughly 50% and 80% as efficient as the parental HCLE cells in gap filling (Fig. 3C). Similarly, MK/T-1 cells infected with Slurp1-expressing adenovirus filled the gap at 50% the pace of control helper virus–infected MK/T-1 cells (Fig. 3D). Together, these results suggest that SLURP1 has a suppressive effect on gap filling by cell migration.

SLURP1 Interacts With uPA

In order to understand the mechanism by which Slurp1 functions, we sought to identify Slurp1-interacting proteins. Ligand blots, wherein mouse kidney lysate was electrophoretically separated, transferred to nitrocellulose membrane, incubated with Slurp1, and probed with anti-Slurp1 antibody, revealed that several proteins interact with Slurp1 (indicated by * in Fig. 4A). When these blots were stripped of the antibody and reprobed with anti-uPA antibody, overlapping bands that aligned with Slurp1-bound protein bands were detected, suggesting that uPA is among the Slurp1-interacting proteins (indicated by ** in Fig. 4A). Pull-down assays, wherein His-Slurp1 or negative control MBP-Slurp1 was bound on Ni-ion resin and incubated with kidney lysate (as a source of uPA), and bound proteins were separated by SDS-PAGE and Slurp1-bound uPA was detected by anti-uPA antibody, confirmed that Slurp1 binds uPA (Fig. 4B). Finally, ELISAs, wherein the wells were coated with MBP or MBP-Slurp1 and bound with MBP or MBP-uPA fusion protein, mock-cleaved MBP or factor Xa–cleaved MBP-uPA, or mouse kidney lysate, confirmed the interaction of mouse Slurp1 with mouse uPA (Fig. 4C, i–iii). Consistent with these results, recombinant human SLURP1 interacted with recombinant human uPA (Fig. 4C, iv). Together, these results identify uPA as one of the SLURP1-binding proteins. The identity of the remaining Slurp1-binding proteins in ligand blots remains to be established.

Slurp1 Decreases the Amount of Cell Surface–Bound uPA at the Leading Edge

Next, we sought to determine the effect of overexpression of SLURP1 on interaction of uPA with its cell-surface receptors. We performed immunofluorescent staining with anti-uPA or anti-SLURP1 antibody 4 hours after gap formation in confluent HCLE or HCLE-SLURP1 cells grown on vitronectin-coated coverslips and treated with 50 U/mL recombinant human uPA. Relatively more uPA was detected in the intercellular margins and the migrating edges of the wild-type HCLE cells compared with the HCLE-SLURP1 cells (Fig. 5A). Consistent with this finding, relatively more uPA was detected at the

moving edge in control protein–treated MK/T-1 cells compared with those treated with Slurp1 (Fig. 5B). Together, these results suggest that SLURP1 decreases the amount of cell surface–bound uPA at the leading edge.

SLURP1 Blocks the Stimulatory Effect of uPA on Cell Migration

In order to determine the functional relevance of SLURP1-uPA interaction, we performed gap-filling assays with HCLE, HCLE–SLURP1-7 and -14 cells, in the presence or absence of 50 U/mL recombinant human uPA (Supplemental Video 1). Treatment of wild-type HCLE cells with uPA resulted in faster gap closure compared with the untreated cells (Fig. 6A). Similar stimulation was not observed in HCLE-SLURP1 cells (Fig. 6B). Measurement of the mean area closed, based on values from six different regions in each treatment confirmed these results (Fig. 6C). Tracking individual cell movement by live-cell microscopy also revealed that the uPA-treated HCLE cells migrated at a significantly higher mean velocity compared with the control, untreated HCLE cells (Fig. 6D). A similar increase was not observed in uPA-treated HCLE-SLURP1 cells, suggesting that SLURP1 blocks the stimulatory effect of uPA on cell migration (Fig. 6D; Supplemental Video 1).

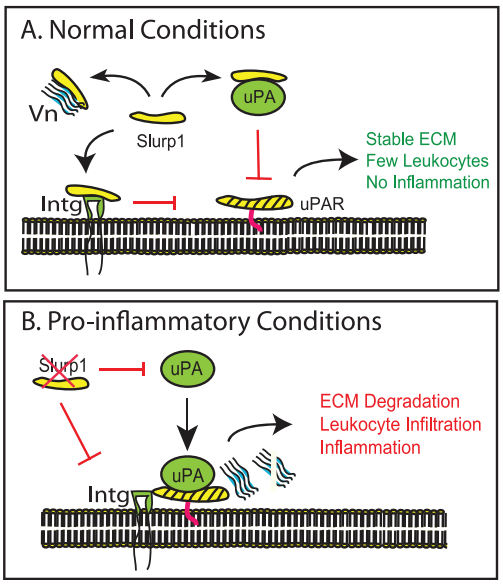

Figure 7. Proposed mechanism by which SLURP1 regulates corneal homeostasis. Data presented in this report suggest that SLURP1 serves as a soluble scavenger of uPA, blocking the essential uPA-dependent functions of uPAR in ECM degradation, leukocyte infiltration, and inflammation.

Discussion

Although Slurp1 is expressed abundantly in the mouse cornea,[24] where it serves an important immunomodulatory role,[15] not much is known about its cellular functions or the mechanism(s) by which it functions. Previous efforts in this direction were largely focused on characterizing SLURP1 activities in oral mucosal epithelial cells or skin keratinocytes as a ligand for α7 nicotinic acetylcholine receptor.[19–21,23,31,33,39,40] However, most studies to date have described muscarinic, but not nicotinic acetylcholine receptors in the cornea.[41–47] Considering that (1) the highly abundantly expressed SLURP1[24] is unlikely to serve as a ligand for nAchRs that are either absent or expressed at low levels in the cornea,[41–47] and (2) the secreted SLURP1 is structurally similar to the membrane-tethered uPAR, which plays essential roles in cellular interaction with the surrounding ECM, we hypothesized that SLURP1 modulates the functions of membrane-tethered uPAR by acting as a soluble scavenger of its ligand uPA, analogous to the role of soluble VEGF receptor in blocking corneal angiogenesis.[8] In this report, we provide evidence that (1) when overexpressed, SLURP1 suppresses the rates of cell proliferation and migration, and (2) SLURP1 functions as a competing soluble scavenger of uPA, blocking the essential uPA-dependent functions of uPAR (Fig. 7).[34,48,49]

The uPA/uPAR system has emerged as a versatile regulator of cell survival, proliferation, migration, adhesion, and differentiation in diverse tissues and physiological contexts.[34,50] Expression of uPAR is sharply elevated in a wide variety of proinflammatory conditions including migrating dermal keratinocytes and placental trophoblasts during tissue remodeling,[51] *Borrelia burgdorferi* infection,[52,53] rheumatic disorders,[54] pemphigus skin blistering,[55] renal dysfunction,[56] atherosclerotic coronary arteries,[57] Kaposi's sarcoma,[58] pathologic angiogenesis,[59] and in leukocytes upon bacterial- or human immunodeficiency virus–1 infection.[52,60] Gradients of uPA are chemotactic for uPAR-expressing cells.[61] Although uPAR facilitates phagocytosis and clearance of *B. burgdorferi* from the heart by a mechanism that is independent of its binding uPA,[53] and uPAR-mediated neutrophil recruitment is independent of uPA,[38,62] other activities of uPAR such as its interaction with vitronectin and β1-integrin, and bacterial clearance, are dependent on uPA.[38,63–65] Regulators such as plasminogen activator inhibitors-1 and -2 (PAI1 and PAI2), α2-anti-plasmin, and maspin fine-tune the uPA/uPAR system by virtue of their ability to block uPA/uPAR interactions. Evidence presented here suggests that SLURP1 plays a similar role as other regulators of the uPA/uPAR system (Fig. 7). It would be worth examining if application of exogenous SLURP1 can block the chemotactic activity of the uPA/uPAR system, facilitating effective management of tissue inflammation in diverse contexts.

Ligand blots revealed that Slurp1 interacts with several proteins, one of which was identified to be uPA (Fig. 4). Though uPA is well established as a ligand for uPAR, many of its functions are independent of binding to uPAR. Experiments using genetically modified mouse strains, in which uPA/uPAR interaction was selectively abrogated retaining their other functions, revealed the role of the uPA/uPAR interaction in cell-associated fibrin surveillance and suppressing chronic inflammation secondary to fibrin deposition, without affecting leukocyte recruitment.[38] The identity of the remaining Slurp1-binding proteins remains to be established. Just as PAI1 binds uPA as well as vitronectin,[66,67] it would be interesting to determine if the remaining unidentified Slurp1-binding proteins are represented among other uPAR ligands.[34]

Overexpression of SLURP1 resulted in decreased rate of proliferation as well as slower gap filling. The possibility that the decreased gap-filling ability of HCLE-SLURP1 cells is an outcome of their lower rate of proliferation is ruled out because the individual HCLE-SLURP1 cells tracked by live-cell microscopy migrated shorter distances at a reduced velocity, compared with the control HCLE cells (Figs. 3, 6). Coupled with the data demonstrating efficient interaction between SLURP1 and uPA (Fig. 4), these results suggest that SLURP1 binds uPA and blocks its stimulatory effects on migration of SLURP1-expressing cells. In order to gain a better understanding of the SLURP1-mediated regulation of uPAR

functions, it would be necessary to quantify and compare the relative affinities of uPA-uPAR and uPA-SLURP1 interactions.

To summarize, the data presented in this report demonstrate that SLURP1 functions as a competing soluble scavenger of uPA. In view of the tissue diversity of uPA/uPAR expression and the broad nature of their functions, it is likely that the involvement of SLURP1 in regulating the uPA/uPAR system also is widespread. For example, anti-uPAR antibody efficiently blocked corneal angiogenesis, leading to the proposal that activation of uPAR upon interaction with uPA is an "angiogenic switch" in the cornea.[68] It is conceivable that SLURP1 presented in high levels in a normal cornea serves an anti-angiogenic role by blocking uPA/uPAR interaction. Sharp downregulation of Slurp1 during alkali burn- or suture-induced corneal neovascularization[30] is consistent with this possibility, which remains to be tested.

Acknowledgments

We thank Ilene Gipson, PhD, Harvard University, and Winston Kao, PhD, University of Cincinnati, for providing HCLE and MK/T-1 cells, respectively; Emili Delp for help in generating SLURP1-expressing stable clones; Kira Lathrop (Imaging Core Facility), for help with imaging; Paul Kinchington, PhD (Molecular Biology Core Facility), and Kate Davoli (Histology Core Facility) for generating adenoviral vectors; and Robert Sobol, PhD, University of Pittsburgh Cancer Institute, for generating the lentiviral vector.

Supported by National Institutes of Health (NIH) Grants: R01EY022898 (SKS) and National Eye Institute core Grant P30 EY08098; by unrestricted grants from Research to Prevent Blindness and the Eye and Ear Foundation of Pittsburgh; and by startup funds from the Department of Ophthalmology, University of Pittsburgh (SKS). Support for the UPCI Lentiviral Facility was provided by the Cancer Center Support Grant P30 CA047904 from the NIH.

Disclosure: **S. Swamynathan** (P); **S.K. Swamynathan** (P)

References

1. Hazlett LD, Hendricks RL. Reviews for immune privilege in the year 2010: immune privilege and infection. *Ocul Immunol Inflamm*. 2010;18:237–243.
2. Niederkorn JY, Stein-Streilein J. History and physiology of immune privilege. *Ocul Immunol Inflamm*. 2010;18:19–23.
3. Azar DT. Corneal angiogenic privilege: angiogenic and antiangiogenic factors in corneal avascularity, vasculogenesis, and wound healing (an American Ophthalmological Society thesis). *Trans Am Ophthalmol Soc*. 2006;104:264–302.
4. Barabino S, Chen Y, Chauhan S, Dana R. Ocular surface immunity: homeostatic mechanisms and their disruption in dry eye disease. *Prog Retin Eye Res*. 2012;31:271–285.
5. Clements JL, Dana R. Inflammatory corneal neovascularization: etiopathogenesis. *Semin Ophthalmol*. 2011;26:235–245.
6. Yamanaka O, Liu CY, Kao WW. Fibrosis in the anterior segments of the eye. *Endocr Metab Immune Disord Drug Targets*. 2010;10:331–335.
7. Gronert K. Resolution, the grail for healthy ocular inflammation. *Exp Eye Res*. 2010;91:478–485.
8. Ambati BK, Nozaki M, Singh N, et al. Corneal avascularity is due to soluble VEGF receptor-1. *Nature*. 2006;443:993–997.
9. Cursiefen C, Chen L, Saint-Geniez M, et al. Nonvascular VEGF receptor 3 expression by corneal epithelium maintains avascularity and vision. *Proc Natl Acad Sci U S A*. 2006;103:11405–11410.
10. Stuart PM, Pan F, Plambeck S, Ferguson TA. FasL-Fas interactions regulate neovascularization in the cornea. *Invest Ophthalmol Vis Sci*. 2003;44:93–98.
11. Morris JE, Zobell S, Yin XT, et al. Mice with mutations in Fas and Fas ligand demonstrate increased herpetic stromal keratitis following corneal infection with HSV-1. *J Immunol*. 2012;188:793–799.
12. Jin Y, Chauhan SK, El Annan J, Sage PT, Sharpe AH, Dana R. A novel function for programmed death ligand-1 regulation of angiogenesis. *Am J Pathol*. 2011;178:1922–1929.
13. El Annan J, Goyal S, Zhang Q, Freeman GJ, Sharpe AH, Dana R. Regulation of T-cell chemotaxis by programmed death-ligand 1 (PD-L1) in dry eye-associated corneal inflammation. *Invest Ophthalmol Vis Sci*. 2010;51:3418–3423.
14. Tandon A, Tovey JC, Sharma A, Gupta R, Mohan RR. Role of transforming growth factor Beta in corneal function, biology and pathology. *Curr Mol Med*. 2010;10:565–578.
15. Swamynathan S, Buela KA, Kinchington P, et al. Klf4 regulates the expression of Slurp1, which functions as an immunomodulatory peptide in the mouse cornea. *Invest Ophthalmol Vis Sci*. 2012;53:8433–8446.
16. Grando SA. Basic and clinical aspects of non-neuronal acetylcholine: biological and clinical significance of non-canonical ligands of epithelial nicotinic acetylcholine receptors. *J Pharmacol Sci*. 2008;106:174–179.
17. Mazar AP. Urokinase plasminogen activator receptor choreographs multiple ligand interactions: implications for tumor progression and therapy. *Clin Cancer Res*. 2008;14:5649–5655.
18. Adermann K, Wattler F, Wattler S, et al. Structural and phylogenetic characterization of human SLURP-1, the first secreted mammalian member of the Ly-6/uPAR protein superfamily. *Protein Sci*. 1999;8:810–819.
19. Moriwaki Y, Yoshikawa K, Fukuda H, Fujii YX, Misawa H, Kawashima K. Immune system expression of SLURP-1 and SLURP-2, two endogenous nicotinic acetylcholine receptor ligands. *Life Sci*. 2007;80:2365–2368.
20. Horiguchi K, Horiguchi S, Yamashita N, et al. Expression of SLURP-1, an endogenous alpha7 nicotinic acetylcholine receptor allosteric ligand, in murine bronchial epithelial cells. *J Neurosci Res*. 2009;87:2740–2747.
21. Moriwaki Y, Watanabe Y, Shinagawa T, et al. Primary sensory neuronal expression of SLURP-1, an endogenous nicotinic acetylcholine receptor ligand. *Neurosci Res*. 2009;64:403–412.
22. Mastrangeli R, Donini S, Kelton CA, et al. ARS Component B: structural characterization, tissue expression and regulation of the gene and protein (SLURP-1) associated with Mal de Meleda. *Eur J Dermatol*. 2003;13:560–570.
23. Arredondo J, Chernyavsky AI, Grando SA. SLURP-1 and -2 in normal, immortalized and malignant oral keratinocytes. *Life Sci*. 2007;80:2243–2247.
24. Norman B, Davis J, Piatigorsky J. Postnatal gene expression in the normal mouse cornea by SAGE. *Invest Ophthalmol Vis Sci*. 2004;45:429–440.
25. Favre B, Plantard L, Aeschbach L, et al. SLURP1 is a late marker of epidermal differentiation and is absent in Mal de Meleda. *J Invest Dermatol*. 2007;127:301–308.
26. Swamynathan S, Kenchegowda D, Piatigorsky J, Swamynathan SK. Regulation of corneal epithelial barrier function by Kruppel-like transcription factor 4. *Invest Ophthalmol Vis Sci*. 2011;52:1762–1769.
27. Swamynathan SK, Davis J, Piatigorsky J. Identification of candidate Klf4 target genes reveals the molecular basis of the diverse regulatory roles of Klf4 in the mouse cornea. *Invest Ophthalmol Vis Sci*. 2008;49:3360–3370.
28. Swamynathan SK, Katz JP, Kaestner KH, Ashery-Padan R, Crawford MA, Piatigorsky J. Conditional deletion of the mouse

Klf4 gene results in corneal epithelial fragility, stromal edema, and loss of conjunctival goblet cells. *Mol Cell Biol*. 2007;27:182–194.

29. Narumoto O, Horiguchi K, Horiguchi S, et al. Down-regulation of secreted lymphocyte antigen-6/urokinase-type plasminogen activator receptor-related peptide-1 (SLURP-1), an endogenous allosteric alpha7 nicotinic acetylcholine receptor modulator, in murine and human asthmatic conditions. *Biochem Biophys Res Commun*. 2010;398:713–718.
30. Jia C, Zhu W, Ren S, Xi H, Li S, Wang Y. Comparison of genome-wide gene expression in suture- and alkali burn-induced murine corneal neovascularization. *Mol Vis*. 2011;17:2386–2399.
31. Arredondo J, Chernyavsky AI, Webber RJ, Grando SA. Biological effects of SLURP-1 on human keratinocytes. *J Invest Dermatol*. 2005;125:1236–1241.
32. Arredondo J, Chernyavsky AI, Grando SA. Overexpression of SLURP-1 and -2 alleviates the tumorigenic action of tobacco-derived nitrosamine on immortalized oral epithelial cells. *Biochem Pharmacol*. 2007;74:1315–1319.
33. Chimienti F, Hogg RC, Plantard L, et al. Identification of SLURP-1 as an epidermal neuromodulator explains the clinical phenotype of Mal de Meleda. *Hum Mol Genet*. 2003;12:3017–3024.
34. Smith HW, Marshall CJ. Regulation of cell signalling by uPAR. *Nat Rev Mol Cell Biol*. 2010;11:23–36.
35. Yang X, Boehm JS, Yang X, et al. A public genome-scale lentiviral expression library of human ORFs. *Nat Methods*. 2011;8:659–661.
36. Gipson IK, Spurr-Michaud S, Argueso P, Tisdale A, Ng TF, Russo CL. Mucin gene expression in immortalized human corneal-limbal and conjunctival epithelial cell lines. *Invest Ophthalmol Vis Sci*. 2003;44:2496–2506.
37. Gendron RL, Liu CY, Paradis H, Adams LC, Kao WW. MK/T-1, an immortalized fibroblast cell line derived using cultures of mouse corneal stroma. *Mol Vis*. 2001;7:107–113.
38. Connolly BM, Choi EY, Gardsvoll H, et al. Selective abrogation of the uPA-uPAR interaction in vivo reveals a novel role in suppression of fibrin-associated inflammation. *Blood*. 2010;116:1593–1603.
39. Chernyavsky AI, Arredondo J, Galitovskiy V, Qian J, Grando SA. Upregulation of nuclear factor-kappaB expression by SLURP-1 is mediated by alpha7-nicotinic acetylcholine receptor and involves both ionic events and activation of protein kinases. *Am J Physiol Cell Physiol*. 2010;299:C903–C911.
40. Chernyavsky AI, Kalantari-Dehaghi M, Phillips C, Marchenko S, Grando SA. Novel cholinergic peptides SLURP-1 and -2 regulate epithelialization of cutaneous and oral wounds. *Wound Repair Regen*. 2011;20:103–113.
41. Tamaddonfard E, Hamzeh-Gooshchi N. Effects of subcutaneous and intracerebroventricular injection of physostigmine on the acute corneal nociception in rats. *Pharmacol Rep*. 2010;62:858–863.
42. Walkenbach RJ, Ye GS. Muscarinic cholinoceptor regulation of cyclic guanosine monophosphate in human corneal epithelium. *Invest Ophthalmol Vis Sci*. 1991;32:610–615.
43. Liu S, Li J, Tan DT, Beuerman RW. Expression and function of muscarinic receptor subtypes on human cornea and conjunctiva. *Invest Ophthalmol Vis Sci*. 2007;48:2987–2996.
44. Grueb M, Mielke J, Bartz-Schmidt KU, Rohrbach JM. Muscarinic cholinoceptor-stimulated phosphatidyl inositol pathway in corneal epithelial and endothelial cells. *Graefes Arch Clin Exp Ophthalmol*. 2007;245:595–599.
45. Grueb M, Reinthal E, Rohrbach JM, Bartz-Schmidt KU. Muscarinic acetylcholine receptor subtypes in human corneal epithelium and endothelium. *Graefes Arch Clin Exp Ophthalmol*. 2006;244:1191–1195.
46. Socci RR, Tachado SD, Aronstam RS, Reinach PS. Characterization of the muscarinic receptor subtypes in the bovine corneal epithelial cells. *J Ocul Pharmacol Ther*. 1996;12:259–269.
47. Lind GJ, Cavanagh HD. Identification and subcellular distribution of muscarinic acetylcholine receptor-related proteins in rabbit corneal and Chinese hamster ovary cells. *Invest Ophthalmol Vis Sci*. 1995;36:1492–1507.
48. Gyetko MR, Sud S, Kendall T, Fuller JA, Newstead MW, Standiford TJ. Urokinase receptor-deficient mice have impaired neutrophil recruitment in response to pulmonary Pseudomonas aeruginosa infection. *J Immunol*. 2000;165:1513–1519.
49. Rijneveld AW, Levi M, Florquin S, Speelman P, Carmeliet P, van Der Poll T. Urokinase receptor is necessary for adequate host defense against pneumococcal pneumonia. *J Immunol*. 2002;168:3507–3511.
50. Blasi F, Carmeliet P. uPAR: a versatile signalling orchestrator. *Nat Rev Mol Cell Biol*. 2002;3:932–943.
51. Solberg H, Ploug M, Hoyer-Hansen G, Nielsen BS, Lund LR. The murine receptor for urokinase-type plasminogen activator is primarily expressed in tissues actively undergoing remodeling. *J Histochem Cytochem*. 2001;49:237–246.
52. Coleman JL, Gebbia JA, Benach JL. Borrelia burgdorferi and other bacterial products induce expression and release of the urokinase receptor (CD87). *J Immunol*. 2001;166:473–480.
53. Hovius JW, Bijlsma MF, van der Windt GJ, et al. The urokinase receptor (uPAR) facilitates clearance of Borrelia burgdorferi. *PLoS Pathog*. 2009;5:e1000447.
54. Del Rosso M, Fibbi G, Matucci Cerinic M. The urokinase-type plasminogen activator system and inflammatory joint diseases. *Clin Exp Rheumatol*. 1999;17:485–498.
55. Xue W, Hashimoto K, Toi Y. Functional involvement of urokinase-type plasminogen activator receptor in pemphigus acantholysis. *J Cutan Pathol*. 1998;25:469–474.
56. Florquin S, van den Berg JG, Olszyna DP, et al. Release of urokinase plasminogen activator receptor during urosepsis and endotoxemia. *Kidney Int*. 2001;59:2054–2061.
57. Okada SS, Golden MA, Raghunath PN, et al. Native atherosclerosis and vein graft arterialization: association with increased urokinase receptor expression in vitro and in vivo. *J Thromb Haemost*. 1998;80:140–147.
58. Thewes M, Elsner E, Wessner D, Engst R, Ring J. The urokinase plasminogen activator system in angiosarcoma, Kaposi's sarcoma, granuloma pyogenicum, and angioma: an immunohistochemical study. *Int J Dermatol*. 2000;39:188–191.
59. Carmeliet P, Jain RK. Angiogenesis in cancer and other diseases. *Nature*. 2000;407:249–257.
60. Speth C, Pichler I, Stockl G, Mair M, Dierich MP. Urokinase plasminogen activator receptor (uPAR; CD87) expression on monocytic cells and T cells is modulated by HIV-1 infection. *Immunobiology*. 1998;199:152–162.
61. Resnati M, Guttinger M, Valcamonica S, Sidenius N, Blasi F, Fazioli F. Proteolytic cleavage of the urokinase receptor substitutes for the agonist-induced chemotactic effect. *EMBO J*. 1996;15:1572–1582.
62. Gueler F, Rong S, Mengel M, et al. Renal urokinase-type plasminogen activator (uPA) receptor but not uPA deficiency strongly attenuates ischemia reperfusion injury and acute kidney allograft rejection. *J Immunol*. 2008;181:1179–1189.
63. Nguyen DH, Catling AD, Webb DJ, et al. Myosin light chain kinase functions downstream of Ras/ERK to promote migration of urokinase-type plasminogen activator-stimulated cells in an integrin-selective manner. *J Cell Biol*. 1999;146:149–164.
64. Sidenius N, Andolfo A, Fesce R, Blasi F. Urokinase regulates vitronectin binding by controlling urokinase receptor oligomerization. *J Biol Chem*. 2002;277:27982–27990.

Investigative Ophthalmology & Visual Science

65. Caiolfa VR, Zamai M, Malengo G, et al. Monomer dimer dynamics and distribution of GPI-anchored uPAR are determined by cell surface protein assemblies. *J Cell Biol*. 2007;179:1067–1082.
66. Deng G, Curriden SA, Wang S, Rosenberg S, Loskutoff DJ. Is plasminogen activator inhibitor-1 the molecular switch that governs urokinase receptor-mediated cell adhesion and release? *J Cell Biol*. 1996;134:1563–1571.
67. Wang L, Ly CM, Ko CY, Meyers EE, Lawrence DA, Bernstein AM. uPA binding to PAI-1 induces corneal myofibroblast differentiation on vitronectin. *Invest Ophthalmol Vis Sci*. 2012;53:4765–4775.
68. Fibbi G, Caldini R, Chevanne M, et al. Urokinase-dependent angiogenesis in vitro and diacylglycerol production are blocked by antisense oligonucleotides against the urokinase receptor. *Lab Invest*. 1998;78:1109–1119.

Investigative Ophthalmology & Visual Science